Int J Clin Exp Pathol 2019;12(6):1947-1955
www.ijcep.com /ISSN:1936-2625/IJCEP0094337

Original Article

Z-VRPR-FMK can inhibit the growth and invasiveness of diffuse large B-cell lymphoma by depressing NF-κB activation and MMP expression induced by MALT1

Jianglong Feng[1], Wenxiu Yang[1], Jiarui Wang[2], Zhenhong Pu[1], Ying Han[3], Long Wan[3]

[1]Department of Pathology, Affiliated Hospital, Guizhou Medical University, Guiyang 550001, Guizhou, China; [2]Department of Pathology, Maternal and Child Health Hospital of Guiyang City, Guiyang, Guizhou, China; [3]Department of Pathology, Guizhou Medical University, Guiyang 550025, Guizhou, China

Received March 25, 2019; Accepted April 18, 2019; Epub June 1, 2019; Published June 15, 2019

Abstract: This study aimed to investigate the therapeutic effect of the mucosa-associated lymphoid tissue lymphoma translocation gene 1 (MALT1) on diffuse large B-cell lymphoma (DLBCL) and its underlying molecular mechanism through the application of Z-Val-Arg-Pro-DL-Arg-fluoromethyl ketone (Z-VRPR-FMK). Cultured OCI-LY10 cells and their xenografts in nude mice were treated with Z-VRPR-FMK. The growth and invasiveness of the tumor were observed. The components of the NF-κB signaling pathways, such as P65, MALT1, A20, matrix metalloproteinase 2 (MMP2) and MMP9, were detected using a real-time fluorescent quantitative polymerase chain reaction, immunohistochemical staining, and a Western blot analysis. Z-VRPR-FMK inhibited the growth and invasiveness of OCI-LY10 cells and their xenografts. The increase in the tumor volume was slower in the experimental group than it was in the control group, and the weight of the nude mice was significantly different between the two groups on the 11th and 13th days of treatment. The expression of P65 was significantly lower at the gene level in cultured OCI-LY10 cells and transplanted tumors than in the controls after treatment with Z-VRPR-FMK. The nuclear expression of the P65 protein of xenografts also decreased, but the nuclear expression of the A20 protein followed a reverse pattern. The expressions of the MALT1, MMP2, and MMP9 proteins were lower in the OCI-LY10 cells and transplanted tumors treated with Z-VRPR-FMK compared with the controls. This study indicates that MALT1 might serve as an effective therapeutic target for activated B-cell (ABC)-like DLBCL. Z-VRPR-FMK inhibits the growth and invasiveness of ABC-like DLBCL by depressing the proteolysis of A20, the activation of NF-κB, and the expression of MMP9 and MMP2 induced by the MALT1 protein.

Keywords: Z-VRPR-FMK, lymphoma, MALT1, A20, NFκB, MMPs

Introduction

Diffuse large B-cell lymphoma (DLBCL), an aggressive lymphoma, occupies about 30%-40% of non-Hodgkin lymphomas in adults [1, 2]. DLBCL is also a group of heterogeneous large-cell lymphomas. Of these, DLBCL not otherwise specified is the most common subtype. DLBCL can be divided into at least three subtypes according to the genetic profiles of its presumed cell of origin: (1) germinal center B-cell (GCB)-like DLBCL; (2) activated B-cell (ABC)-like DLBCL; and (3) primary mediastinal large B-cell lymphoma. ABC-like DLBCL has a worse clinical course and prognosis compared with GCB-like DLBCL [3]. Since patients respond differently to common therapy, it is necessary to discover new therapeutic targets for the individualized treatment of DLBCL. The abnormal activation of NF-κB is an important feature of DLBCL, especially ABC-like DLBCL. NF-κB/p65 was found to be overexpressed in the nucleus of ABC-like DLBCL and is associated with a poor prognosis of the tumor [4, 5]. Matrix metalloproteinases (MMPs), a protease family involved in the degradation of the extracellular matrix, is closely related to tumor invasion and metastasis [6, 7]. NF-κB is the transcriptional regulator of MMPs. It can lead to the overexpression of MMPs by binding to the -615 and -600 loci of the MMP promoter [8, 9]. In DLBCL, some recurrent mutations/gene alterations,

such as mucosa-associated lymphoid tissue lymphoma translocation gene 1 (MALT1), tumor necrosis factor, the alpha-induced protein 3 gene (TNFAIP3, A20), the MAGUK family of proteins (CARD II/Carma1/Bimp3), B-cell leukemia/lymphoma 10 (BCL10), and the myeloid differentiation primary response gene (MyD88), are associated with the dysregulation of NF-κB [10, 11]. Finding novel therapeutic targets for DLBCL might be helpful in exploring the genetic features and the relative signal transduction pathway [12]. A previous study reported an up-regulated expression of MATL1 mRNA in DLBCL. The overexpression was associated with the expression of BCL2 and the poor prognosis of DLBCL. The MALT1 protein (also named paracaspase) can activate NF-κB. It phosphorylates the kappa B kinase in several ways such as self-oligomerization, formation of CBM (formation of complexes with membrane-associated ornithine kinase protein-1 and the B-cell leukemia/lymphoma 10 and MALT1) complex [13]. Ubiquitination and the proteolytic effect of MALT1 are also closely related to the activation of NF-κB [14, 15]. A20 is a negative regulator of NF-κB. It can block the upstream signal from the IKKγ subunits to IKKα and IKKβ by interacting with IKKγ, thus blocking the activation of NF-κB. The proteolytic effect of MALT1 on the A20 protein helps in the activation of NF-κB [16]. Therefore, blocking the MALT1 protein may inhibit the activation of NF-κB through multiple mechanisms. Z-Val-Arg-Pro-DL-Arg-fluoromethylketone (Z-VRPR-FMK), a peptide inhibitor, is a tetrapeptide composed of valine, arginine, proline, and arginine. It can suppress the MALT1 protein irreversibly. This study investigated the therapeutic effect of MALT1 on DLBCL and its underlying molecular mechanism using Z-VRPR-FMK.

Materials and methods

Cell culture and treatment

OCI-LY10, an ABC-like DLBCL cell line, were donated by the Laboratory of Hematology of the Affiliated Hospital of Guizhou Medical University. The OCI-LY10 cells were cultured at 37°C in the presence of 5% carbon dioxide in 84% Iscove's modified Dulbecco's medium supplemented with 15% FCS, 1% penicillin, and streptomycin. The cells in the logarithmic phase were collected and adjusted to the appropriate concentration. Then, 80 μL of the cells were inoculated in a 96-well plate. The concentration of the cells was about 1.25×10^5/mL per hole, and the zero hole was set. The cells were placed in an incubator maintained at 37°C, 5% CO_2, and 95% saturated air. They were divided into two groups and treated with 75 mol/L of Z-VRPR-FMK for 6, 12, 24, 36, and 48 h and then fresh serum culture medium successively. Further, 10 μL of MTT solution was added to each hole and incubated in an incubator at 37°C for 4 h. The resulting formazan crystals were dissolved in DMSO. The absorbance was read at 570 nm on a Rayto RT-6000 microplate reader (Rayto Life and Analytical Sciences Co., Ltd., Shenzhen, China).

Transwell migration assay

Biocoat Matrigel invasion chamber inserts (BD Biosciences) were mixed with a serum-free medium (1:9) on ice boxes. The chambers were placed on 24 orifices. A total of 2×10^5 cells from each orifice in the serum-free medium were seeded into the upper chamber of the insert precoated with Matrigel for a migration assay following various treatments (10 μL of Z-VRPR-FMK for the inhibitor group and 10 mL of a non-serum culture medium for the blank control group). Then, 500 μL of the 10% medium was added in the lower chamber. The cells on 24 orifices were incubated overnight at 37°C with 5% CO_2. The inoculated cells were removed and those in the lower chamber were observed under a microscope. The cellular suspension in the lower chamber was moved into 96-well plates and subjected to MTT detection (the absorbance was set at 600 nm).

Model establishment and the treatment of the xenografts of large B-cell lymphoma in nude mice

A total of 8 female BALB/c nude mice of SPF grade (aged 4-6 weeks and weighing 16-20 g) were purchased from Beijing HuaFuKang Biotechnology Company [qualified animal license numbers: SCXK (Beijing), 2014-0004, Certificate of Quality No: 11401300032066]. The experiment was approved by the ethics committee of Guizhou Medical University (document number: No1503004). The BALB/c nude mice were fed in cages sterilized with high-pressure steam. The biological laminar flow rack for these cages was also subjected to UV disinfection on a regular basis. A constant tem-

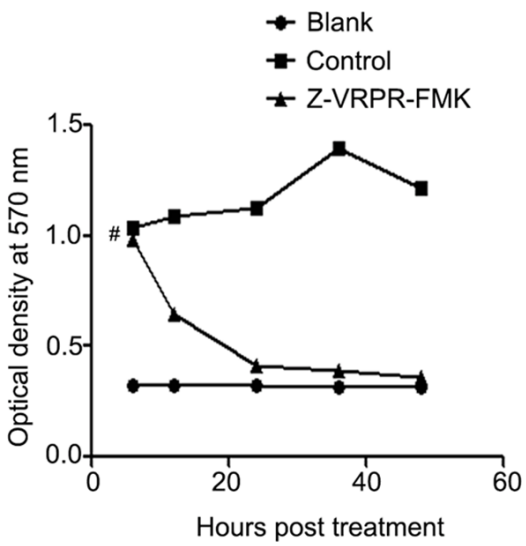

Figure 1. The effect of Z-VRPR-FMK on the growth of OCI-LY10 cells. Values are presented as the mean ± SD. #*P* < 0.01 versus the control group.

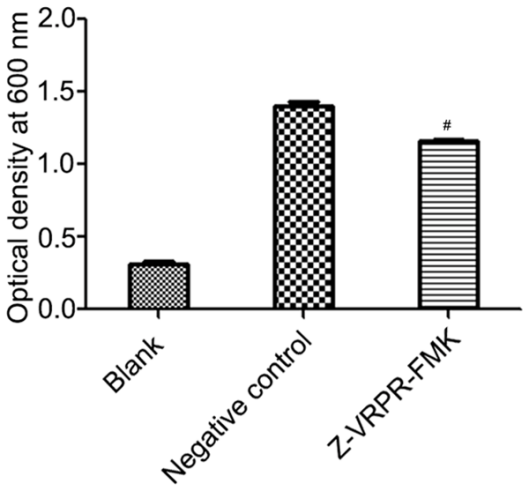

Figure 2. The effect of Z-VRPR-FMK on the invasiveness of OCI-LY10 cells. Values are presented as the mean ± SD. #*P* < 0.01 versus the control group.

perature (about 25°C) and humidity (about 50%) were maintained in the room. The experimental operation was conducted under aseptic conditions after a week of adaptive feeding and several days of pretreatment with an intraperitoneal injection of cyclophosphamide (75 mg/kg; 0.2 mL). The cell suspension concentration of the OCI-LY10 cells in the logarithmic growth phase was adjusted to 2 × 10^7/mL using a serum-free culture medium. Further, 0.2 mL of the suspension was injected subcutaneously into the left forelimbs of all nude mice. The tumor formation was observed at different times, and a tumor growth curve was plotted. After the successful modeling, the animals were divided into experimental and control groups. The two groups of nude mice were injected with 0.2 mL of Z-VRPR-FMK (37.5 M) or saline, respectively, every other day for 12 days. After the aforementioned treatment, these animals were sacrificed, and the transplanted tumors were examined using a morphologic observation, immunohistochemical staining, and a molecular biological examination.

Morphological observation and immunophenotype detection

The morphological changes were observed using traditional hematoxylin and eosin staining. The immunophenotypes were detected using immunohistochemical staining. For this, 4-μm-thick paraffin slices were prepared. The Envision two-step method and DAB, a chromogenic agent, were used after dewaxing, hydration, eliminating endogenous peroxidase, and antigen retrieval. The primary antibodies and their dilutions were as follows: MALT1 (Abcam, 1:100), A20 (Abcam, 1:300), NF-κB (P65, Abcam, 1:100), MMP9/2 (Abcam, 1:100), CD20 (MXB, 1:200), CD10 (MXB, 1:100), BCL6 (MXB, 1:100), and MUM1 (MXB, ready to use). The P65-positive signal was located in the nucleus (activation performance of NFκB), while the other signals were found in the cytoplasms. Ten fields of view (40 × magnification) were randomly selected for counting the positive cells, and the average number of the 10 fields of view denoted the positivity rate. Further, if ≥ 20% cells stained positive, they were arbitrarily considered positive, and if < 20% cells stained positive, they were considered negative for estimating the levels of P65, A20, MALT1, MMP2, and MMP9 proteins.

Quantitative real-time polymerase chain reaction

Total RNA was extracted from the OCL-LY10 cells and the transplanted tumor tissue using TRIzol reagent (Invitrogen, USA) according to the manufacturer's protocol. The purity and concentration of total RNA were determined using a nucleic acid measurement instrument (ND200). Also, cDNA from 0.1-5 ng total RNA was synthesized with the RevertAid M-MuLV

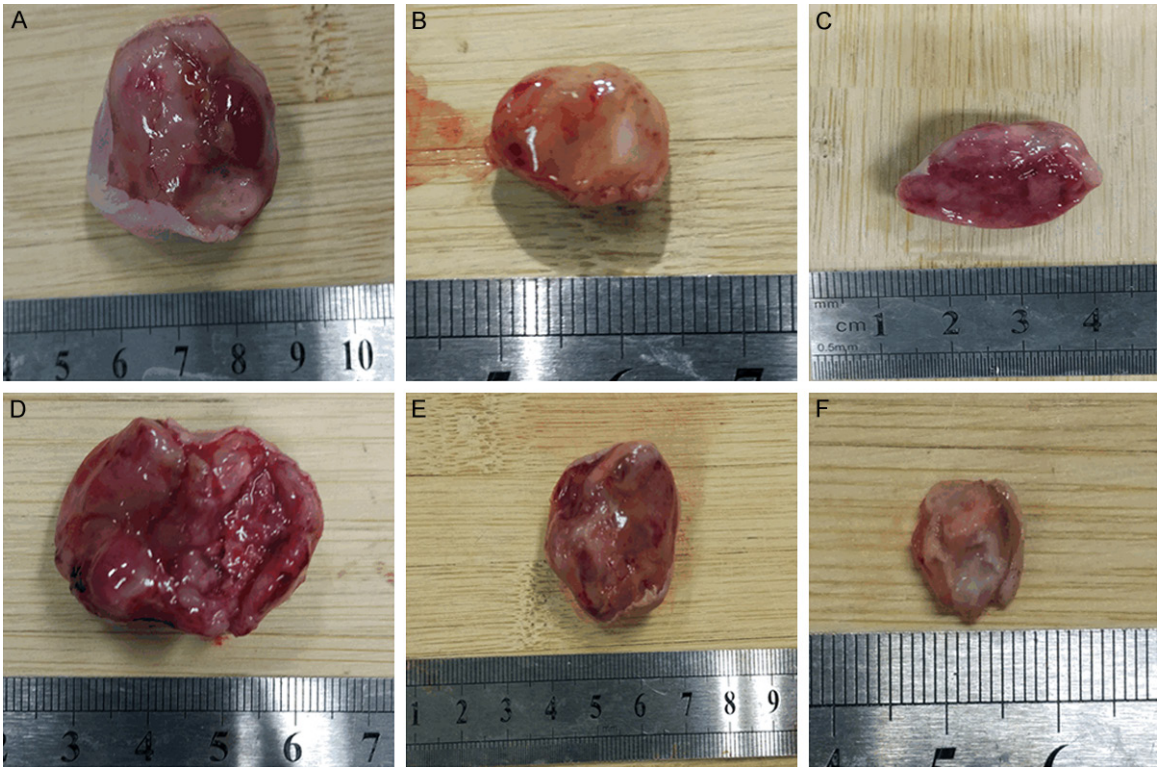

Figure 3. A transplanted tumor of OCI-LY10 cells in nude mice. (A-C) Z-VRPR-FMK groups; and (D-F) control groups.

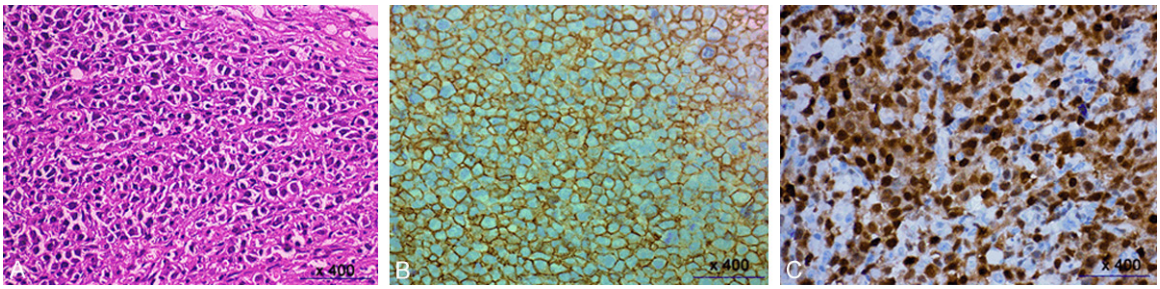

Figure 4. The morphology and immunophenotypes of the transplanted tumor of OCI-LY10 cells in nude mice. (A) Morphology (HE, × 400), (B) expression of CD20 (Envision, × 400), and (C) expression of MUM-1 (Envision, × 400).

reverse transcriptase (Invitrogen). A quantitative real-time polymerase chain reaction (PCR) was performed using a reaction system of 20 μL as follows: 1 μL (100 ng) of the template, 10 μL of SYBR Green, 10 μM (1 μL) of each primer (forward and reverse), and nuclease-free water to a final volume of 20 μL. The primers were designed using Premier 5.0. GAPDH was used as an internal control. The primer sequences were as follows: P65 (5'-ATGTGGAGATCATTGAGCAGC-3', 5'-CCTGGTCCTGTGTAGCCATT-3'); GAPDH (5'-TGGACTCCACGACGTACTCAG-3', 5'-ACATGTTCCAATATGATTCCA-3'). PCR was performed on an ABI Real-Time PCR system 7500 Fast Thermal Cycler (Applied Biosystems, Inc., USA). The cycling conditions were as follows: 95°C for 10 min, 40 cycles of 95°C for 30 s, 60°C for 30 s, 72°C for 40 s, and eventually 72°C for 5 min. Data were analyzed using the Sequence Detection Software version 1.6.3 supplied by Applied Biosystems. The comparative cycle threshold (ΔΔCt) method was adopted for quantitation.

Western blot analysis

To prepare the protein extracts, OCI-LY10 cells (3×10^6) or 100 mg tumor tissues were fully lysed with a RIPA buffer on ice for 15 min. These lysed cells or tissues were centrifuged at

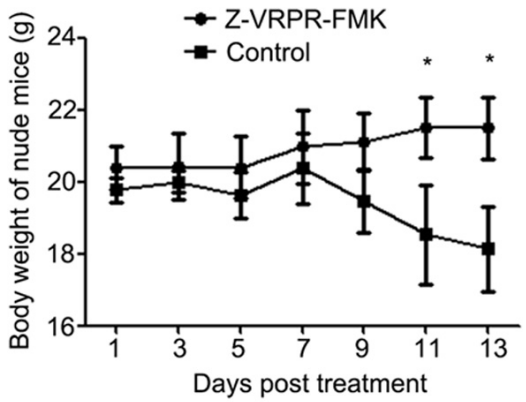

Figure 5. A curve of the body weight change of nude mice. Values are presented as the mean ± SD. *P < 0.05 versus the control group.

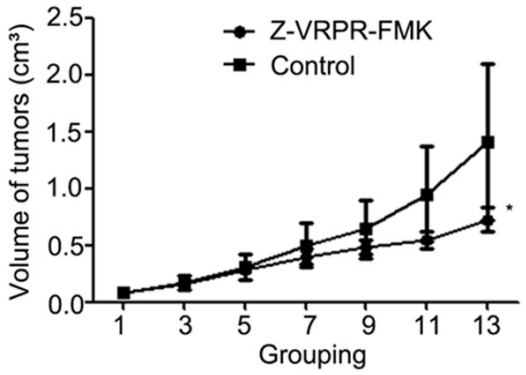

Figure 6. Curves of the volume change of transplanted tumors in nude mice. Values are presented as the mean ± SD. *P < 0.05 versus the control group.

12,000 rpm at 4°C for 20 min. The supernatants were collected, and the protein concentration was determined using a colorimetric BCA protein assay. Further, 80 μL of total protein for each sample was resolved in 12% sodium dodecyl sulfate-polyacrylamide gel electrophoresis. The proteins were electroblotted onto polyvinylidene fluoride membranes, blocked with 5% skimmed milk powder for 1 h at room temperature, and washed with TBST three times for 5 min. Then, primary antibodies (1:1000 of mouse anti-MALT1 polyclonal antibody, 1:500 of mouse anti-TNFAIP3 monoclonal antibody, 1:1000 of MMP9, and 1:1000 of MMP2, all purchased from Abcam) were added overnight at 4°C. Also, β-actin (1:3000, from Santa Cruz Co., Ltd.) was used as an internal control. The treated membranes were washed three times with TBST, incubated for 1 h at room temperature with a goat anti-mouse IgG or goat anti-rabbit IgG secondary antibody (1:3000, from Beijing Changsheng Biotechnology Company), and washed again with TBST. Finally, a Western blot analysis was conducted with enhanced chemiluminescence. Quantitative analysis was performed with Image-Pro Plus analysis software (Media Cybernetics).

Statistical analysis

All the data were analyzed using the SPSS 19.0 statistical software package (SPSS, USA). The experiments were repeated three times. The values were reported as the mean ± standard deviation (SD). Tests for the homogeneity of variance were performed before the analysis of variance. A one-way analysis of variance was used according to the data characteristics. A P value less than 0.05 was considered to indicate a statistically significant result.

Results

Z-VRPR-FMK inhibited the proliferation and migration of OCI-LY10 cells

Cell proliferation was inhibited after 6-h treatment with Z-VRPR-FMK. The cell viability was clearly decreased in the experimental group compared with the control group after 12-h treatment with Z-VRPR-FMK. However, the proliferation was not inhibited in a time-dependent manner (P < 0.01, **Figure 1**). As shown in **Figure 2**, the optical density of the cells was significantly lower in the inhibitor group at 600 nm wavelength than they were in the control group (1.165±0.007 vs 1.404±0.031; P < 0.01). The result indicated that the invasiveness of OCI-LY10 was weakened in the treated group compared with the control group.

Morphology and immunophenotypes of xenografts of OCI-LY10 cells in nude mice

An *in vivo* experiment showed that the tumor mass could be felt in nude mice 14 days after inoculation, and the tumor formation rate of the OCI-LY10 cells was 75% (6/8), as shown in **Figure 3**. Grossly, the xenografts were found to have clearly bounded nodules without a capsule. Histologically, the tumor presented a diffuse growth pattern. The tumor cells were large and round. The nuclei were round or oval, with vacuolar chromatins, distinct nucleoli, and thick nuclear membranes. The cytoplasms were bichromatic or chromophilic. The immuno-

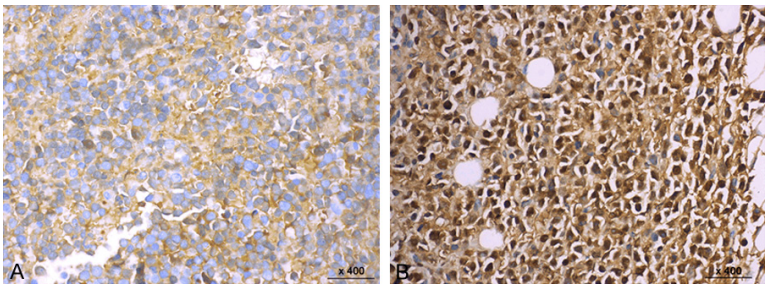

Figure 7. The expression of the P65 protein in the xenografts of OCI-LY10 cells (Envision, × 400). A. Inhibitor group; B. Control group.

phenotypes of the tumor cells were as follows: CD10 (-), CD20 (+), MUM1 (+), BCL6 (+), CD3 (-), and CD5 (-), as shown in **Figure 4**.

Z-VRPR-FMK inhibited the growth of the xenografts of OCI-LY10 cells in nude mice

As shown in **Figure 5**, the weight of the nude mice increased after stimulation with Z-VRPR-FMK. The control group gradually lost weight after 9 days, but the weight of the experimental group increased continuously. A significant difference in the weight was found between the two groups on the 11th and 13th days of treatment ($P < 0.05$). The increase in the size of the tumor was slower in the experimental group than it was in the control group after the 13th day of drug treatment (0.800±0.177 vs 1.445±1.016; $P < 0.05$; **Figure 6**).

Z-VRPR-FMK decreased the expression of P65

The expression of P65 mRNA was significantly lower in the OCI-LY10 cells treated with Z-VRPR-FMK for 12 h compared with the control group (0.227±0.035 vs 1; $P < 0.01$). The change pattern was similar in the xenografts of OCI-LY10 cells (0.62±0.012 vs 1; $P < 0.01$). The positive expression of the p65 protein in the nuclei suggested NF-κB activation. The positive expression rate was 100% and 0 in the control and experimental groups, respectively. The difference in the expression of the P65 protein between the two groups was statistically significant ($P \leq 0.01$; **Figure 7**).

The effect of Z-VRPR-FMK on the expression of some molecules associated with NF-κB activation and MMPs in OCI-LY10 cells and their xenografts

Immunohistochemical staining indicated that four kinds of proteins were expressed in the cytoplasms of the tumor cells. The expressions of various proteins in the inhibitor and control groups (control vs inhibitor) were 1/3:3/3 (A20), 3/3:0/3 (MALT1), 3/3:1/3 (MMP2) and 2/3:0/3 (MMP9) (**Figure 8**).

The Western blot analysis showed that the expression of the A20 protein significantly increased, but the expressions of the MALT1, MMP-2, and MMP-9 proteins decreased in the experimental groups after treatment with Z-VRPR-FMK compared with the cells and xenografts in the control group (**Figures 9** and **10**; $P < 0.05$).

Discussion

R-CHOP, a combination of the anti-CD20 monoclonal antibody rituximab and four chemotherapeutic agents (cyclophosphamide, doxorubicin, vincristine, and prednisolone), is the standard chemo-immunotherapy treatment for DLBCL. However, a considerable number of patients have relapsed/refractory after treatment for DLBCL because of the heterogeneity of DLBCL. MALT1 is an abnormally active gene in DLBCL. It can be overexpressed due to its involvement in the formation of chromosome translocation t(14;18) or genomic amplification; also, some genetic aberrations of A20, such as deletion, point mutation, and methylation, can be found in some patients with DLBCL [10]. As a proteolytic substrate of the MALT1 protein, the A20 protein is degraded, so that its inhibitory effect on NF-κB weakens [17, 18]. Recently, MALT1 protease gained attention as a therapeutic target of DLBCL [19, 20]. Both literature reviews and earlier studies have indicated the effect of MALT1 inhibitors on the growth of ABC-like rather than GCB-like DLBCL cells [19, 21]. In this study, a MALTI inhibitor Z-VRPR-FMK was used to treat cultured OCI-LY10 cells *in vitro* and transplanted tumors in nude mice *in vivo*. Z-VRPR-FMK was found to inhibit the growth of OCI-LY10 cells and their xenografts. The expression of the MALT1 protein also decreased. Z-VRPR-FMK could inhibit the growth of ABC-like DLBCL by restraining the MALT1 protein. The P65 protein expression in nuclei was reduced, but the expression of the A20 protein increased after treatment with Z-VRPR-FMK.

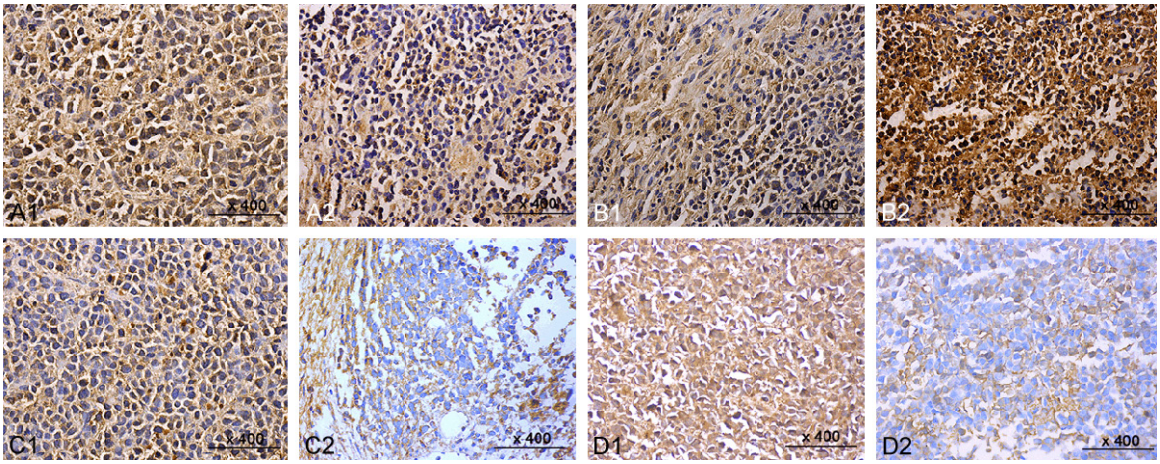

Figure 8. The expressions of various proteins in the xenografts of OCI-LY10 cells (Envision, × 400). (A1, A2) Expression of MALT1 in the control and inhibitor groups, successively; (B1, B2) expression of A20 in the control and inhibitor groups; (C1, C2) expression of MMP2 in the control and inhibitor groups; and (D1, D2) expression of MMP9 in the control and inhibitor groups.

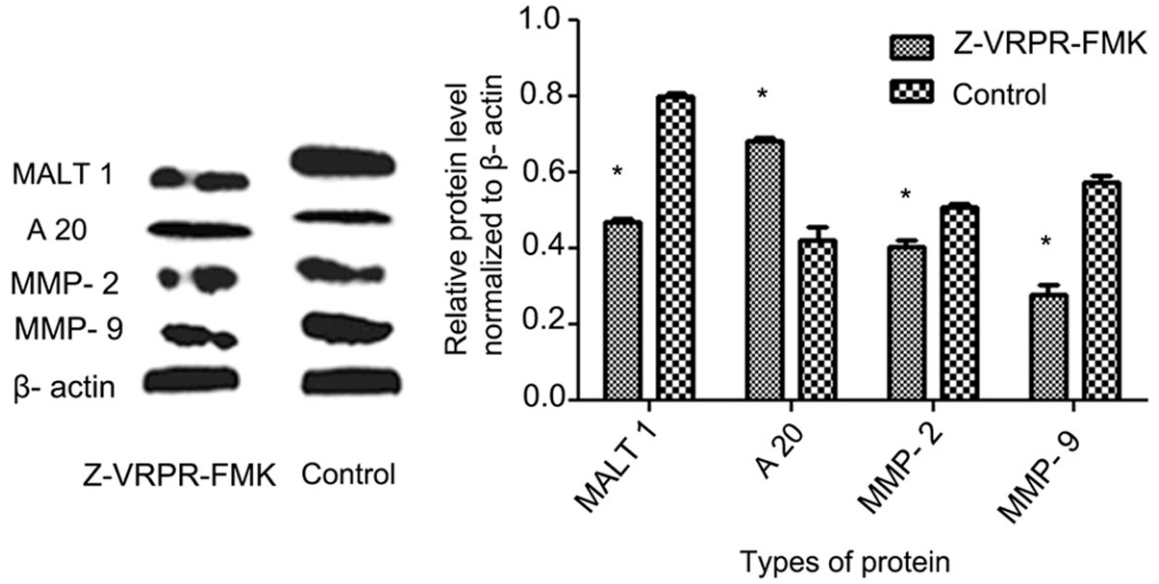

Figure 9. The effects of Z-VRPR-FMK on the expression of A20, MALT1, MMP-2, and MMP-9 in OCI-LY10 cells. Values are presented as the mean ± SD. *$P < 0.05$ versus the control group.

The results suggested that Z-VRPR-FMK could effectively inhibit the activation of NF-κB by directly irreversibly inhibiting the expression of the MALT1 protein. This inhibition of NF-κB activation might be related to weakening or even eliminating the proteolysis of the A20 protein by the MALT1 protein. Meanwhile, the expression of P65 mRNA decreased after treatment with Z-VRPR-FMK, indicating that Z-VRPR-FMK reduced NF-κB activation in DLBCL cells in more than one way by eliminating the proteolytic effect of MALT1 on the A20 protein. As a significant transcriptional factor, NF-κB regulates the expression of several genes involved in cellular proliferation, apoptosis, the cell cycle, and the invasiveness and metastasis of tumors. However, the molecular mechanism underlying the involvement of the NF-κB signaling pathway in the invasiveness and metastasis of DLBCL is still unclear. Some members of the MMP family were found to be regulated by NF-κB. A study demonstrated that MALT1 posi-

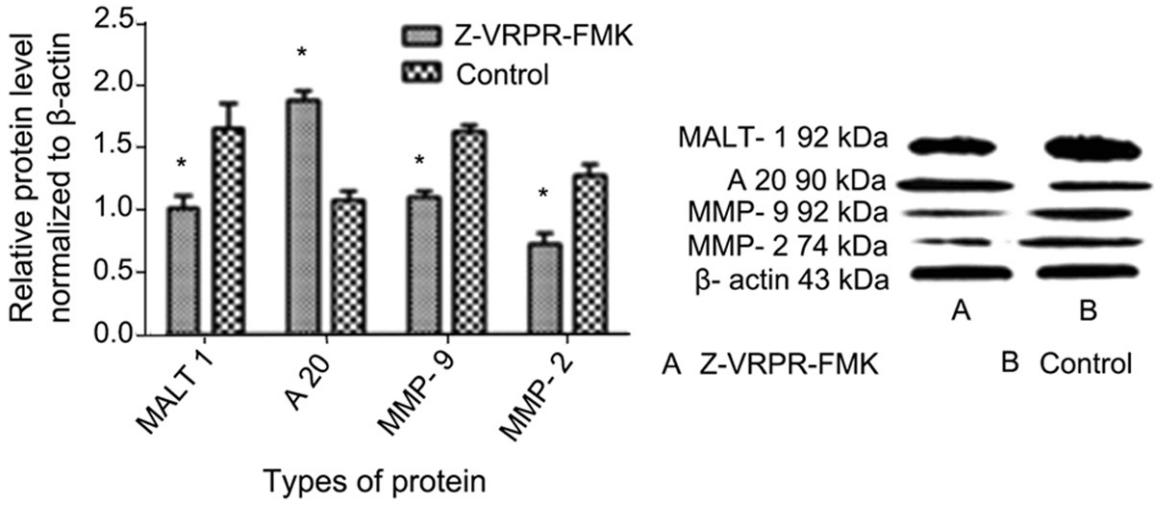

Figure 10. Effects of Z-VRPR-FMK on the expression of A20, MALT1, MMP-2, and MMP-9 in the transplanted tumors of the OCI-LY10 cells in nude mice. Values are presented as the mean ± SD. *$P < 0.05$ versus the control group.

tively modulated MMP9 production in alveolar macrophages [22]. The present study investigated the relationship between Z-VRPR-FMK and the migration of ABC-like DLBCL cells and the expression of MMP2 and MMP9 proteins.

The mobility of the OCI-LY10 cells decreased significantly and the expressions of the MMP-2 and MMP-9 proteins in the OCI-LY10 cells and xenografts reduced significantly after treatment with Z-VRPR-FMK. This finding indicated that Z-VRPR-FMK could prevent the invasiveness of ABC-like DLBCL by controlling the MALT1 protein. This inhibitory action might be related to a reduced expression of MMP2 and MMP9. NF-κB has an important role in the invasiveness of DLBCL cells. MMP2 and MMP9 are possibly the targets of NF-κB in promoting the infiltration of ABC-like DLBCL cells. Whether MALT1 promotes MMP9 and MMP2 expressions in DLBCL needs further confirmation.

In conclusion, the present study demonstrated that Z-VRPR-FMK can inhibit the growth of ABC-like DLBCL, an effect associated with the suppression of the expression of the MALT1 protein. MALT1 may be considered an effective therapeutic target for ABC-like DLBCL. It impacts the growth and invasiveness of DLBCL by boosting the activation of NF-κB. Perhaps Z-VRPR-FMK reduces NF-κB activation. The overexpression of MMP2 and MMP9 was probably induced by NF-κB and may be an important molecular mechanism associated with the infiltration of DLBCL.

Acknowledgements

This study supported by the National Natural Science Foundation of China (no. 81160299).

Disclosure of conflict of interest

None.

Address correspondence to: Dr. Wenxiu Yang, Department of Pathology, Affiliated Hospital of Guizhou Medical University, 9 Beijing Road, Guiyang 550001, Guizhou, China. E-mail: 2916205472@qq.com

References

[1] Korkolopoulou P, Vassilakopoulos T, Milionis V and Ioannou M. Recent advances in aggressive large B-cell lymphomas: a comprehensive review. Adv Anat Pathol 2016; 23: 202-243.

[2] Li S, Young KH and Medeiros LJ. Diffuse large B-cell lymphoma. Pathology 2018; 50: 74-87.

[3] Swerdlow and Steven H. WHO classification of tumours of haematopoietic and lymphoid tissues. Pathologica 2008: 83-87.

[4] Schmitz R, Wright GW, Huang DW, Johnson CA, Phelan JD, Wang JQ, Roulland S, Kasbekar M, Young RM, Shaffer AL, Hodson DJ, Xiao W, Yu X, Yang Y, Zhao H, Xu W, Liu X, Zhou B, Du W, Chan WC, Jaffe ES, Gascoyne RD, Connors JM, Campo E, Lopez-Guillermo A, Rosenwald A, Ott G, Delabie J, Rimsza LM, Tay Kuang Wei K, Zelenetz AD, Leonard JP, Bartlett NL, Tran B, Shetty J, Zhao Y, Soppet DR, Pittaluga S, Wilson WH and Staudt LM. Genetics and pathogenesis of diffuse large B-cell lymphoma. N Engl J Med 2018; 378: 1396-1407.

[5] Niu M, Shen Y, Xu X, Yao Y, Fu C, Yan Z, Wu Q, Cao J, Sang W, Zeng L, Li Z, Liu X and Xu K. Piperlongumine selectively suppresses ABC-DLBCL through inhibition of NF-kappaB p65 subunit nuclear import. Biochem Biophys Res Commun 2015; 462: 326-331.

[6] Zhang QY, Li R, Zeng GF, Liu B, Liu J, Shu Y, Liu ZK, Qiu ZD, Wang DJ, Miao HL, Li MY, Zhu RZ. Dihydromyricetin inhibits migration and invasion of hepatoma cells through regulation of MMP-9 expression. World J Gastroenterol 2014; 20: 10082-10093.

[7] Nishio K, Motozawa K, Omagari D, Gojoubori T, Ikeda T, Asano M and Gionhaku N. Comparison of MMP2 and MMP9 expression levels between primary and metastatic regions of oral squamous cell carcinoma. J Oral Sci 2016; 58: 59-65.

[8] Nichol JW, Gaynor JW and Gooch KJ. Simultaneously reduced hemodynamics and increased axial strain in engineered arteries leads to additive increase in MMP-9 but not MMP-2 expression, mediated by NF-κB subunits p50 and p65. Vascular Pharmacology 2006; 45: 186-187.

[9] Frey AB, Wali A, Pass H and Lonardo F. Osteopontin is linked to p65 and MMP-9 expression in pulmonary adenocarcinoma but not in malignant pleural mesothelioma. Histopathology 2007; 50: 720-726.

[10] Reddy A, Zhang J, Davis NS, Moffitt AB, Love CL, Waldrop A, Leppa S, Pasanen A, Meriranta L, Karjalainen-Lindsberg ML, Norgaard P, Pedersen M, Gang AO, Hogdall E, Heavican TB, Lone W, Iqbal J, Qin Q, Li G, Kim SY, Healy J, Richards KL, Fedoriw Y, Bernal-Mizrachi L, Koff JL, Staton AD, Flowers CR, Paltiel O, Goldschmidt N, Calaminici M, Clear A, Gribben J, Nguyen E, Czader MB, Ondrejka SL, Collie A, Hsi ED, Tse E, Au-Yeung RKH, Kwong YL, Srivastava G, Choi WWL, Evens AM, Pilichowska M, Sengar M, Reddy N, Li S, Chadburn A, Gordon LI, Jaffe ES, Levy S, Rempel R, Tzeng T, Happ LE, Dave T, Rajagopalan D, Datta J, Dunson DB and Dave SS. Genetic and functional drivers of diffuse large B cell lymphoma. Cell 2017; 171: 481-494, e415.

[11] Abubaker J, Bavi P and Jehan Z. Role of NF-κB regulators A20 and CARD11 in middle eastern diffuse large B cell lymphoma. Cancer Res 2011; 71: 4192-4192.

[12] Amin AD, Peters TL, Li L, Rajan SS, Choudhari R, Puvvada SD and Schatz JH. Diffuse large B-cell lymphoma: can genomics improve treatment options for a curable cancer? Cold Spring Harb Mol Case Stud 2017; 3: a001719.

[13] David L, Li Y, Ma J, Garner E, Zhang X and Wu H. Assembly mechanism of the CARMA1-BCL10-MALT1-TRAF6 signalosome. Proc Natl Acad Sci U S A 2018; 115: 1499-1504.

[14] Karim ZA, Vemana HP, Khasawneh FT. MALT1-ubiquitination triggers non-genomic NF-κB/IKK signaling upon platelet activation. PLoS One 2015; 10: e0119363.

[15] Staal J, Bekaert T and Beyaert R. Regulation of NF-kappaB signaling by caspases and MALT1 paracaspase. Cell Res 2011; 21: 40-54.

[16] Ferch U, Kloo B, Gewies A, Pfander V, Duwel M, Peschel C, Krappmann D and Ruland J. Inhibition of MALT1 protease activity is selectively toxic for activated B cell-like diffuse large B cell lymphoma cells. J Exp Med 2009; 206: 2313-2320.

[17] Coornaert B, Baens M, Heyninck K, Bekaert T, Haegman M, Staal J, Sun L, Chen ZJ, Marynen P and Beyaert R. T cell antigen receptor stimulation induces MALT1 paracaspase-mediated cleavage of the NF-kappaB inhibitor A20. Nat Immunol 2008; 9: 263-271.

[18] Turturro F. Constitutive NF-kappa B activation underlines major mechanism of drug resistance in relapsed refractory diffuse large B cell lymphoma. Biomed Res Int 2015; 2015: 484537.

[19] Fontan L, Qiao Q, Hatcher JM, Casalena G, Us I, Teater M, Durant M, Du G, Xia M, Bilchuk N, Chennamadhavuni S, Palladino G, Inghirami G, Philippar U, Wu H, Scott DA, Gray NS and Melnick A. Specific covalent inhibition of MALT1 paracaspase suppresses B cell lymphoma growth. J Clin Invest 2018; 128: 4397-4412.

[20] Jaworski M and Thome M. The paracaspase MALT1: biological function and potential for therapeutic inhibition. Cell Mol Life Sci 2016; 73: 459-473.

[21] Yang WX, Li Y, Li PH and Wang LL. PMA/IONO affects diffuse large B-cell lymphoma cell growth through upregulation of A20 expression. Oncol Rep 2016; 36: 1069-1075.

[22] Lee YH, Huang JH, Chang TH, Yang HC and Wu-Hsieh BA. Mucosa-associated lymphoid tissue lymphoma translocation protein 1 positively modulates matrix metalloproteinase-9 production in alveolar macrophages upon toll-like receptor 7 signaling and influenza virus infection. Front Immunol 2017; 8: 1177.